

# EFFECTS OF GEO-ATMOSPHERIC PREPROCESSING ON IMAGING SPECTROSCOPY DATA QUALITY AND METHODS

Daniel Schläpfer, Philipp Meier, and Michael Schaepman

*Remote Sensing Laboratories (RSL),  
Department of Geography, University of Zurich, CH-8057 Zurich, Switzerland  
Phone: +41 1 635 52 50, Fax: +41 1 635 68 46, E-mail: dschlapf@geo.unizh.ch*

## 1. INTRODUCTION

Advanced methods of geo-atmospheric preprocessing have become available in the past years and increasingly are applied to AVIRIS airborne imagery. Both, the geometric as well as the atmospheric part of the preprocessing have their specific impact on data quality which should be aware to scientists using such corrected data. An integral geo-atmospheric correction has been developed in a joint effort by the Remote Sensing Laboratories of the University of Zurich and the German Aerospace Agency of Wessling, Germany. It combines the parametric orthorectification program PARGE (Schläpfer et al., 1998) with the atmospheric and topographic correction program ATCOR4 (Richter et al. 2000). The method has been successfully tested on AVIRIS and other airborne imaging spectrometry data such as DAIS, HyMap, and CASI. The method has been described in the abovementioned papers and thus is not further explained herein. In the following, two specific radiometric problems inhere to geometric as well as to atmospheric and topographic correction are explained and potential solutions are depicted.

In the first experiment, the impact of spatial resampling on the spectral accuracy is determined by comparing resampled AVIRIS imagery to its original counterparts. The spectral artefacts appearing while applying resampling technologies during the geometric processing lead to conclusions on how to perform geometric resampling in hyperspectral imagery. The comparison of nearest neighbor resampling to interpolation procedures shows how the spectral and spatial accuracy is affected after applying any of these methods in the parametric geometric correction process.

Second, the impact of radiometric processing on the performance of hyperspectral methods such as spectral angle mapping and spectral unmixing is analysed. The tests are performed on AVIRIS low altitude and high altitude over the Ray Mine area in Arizona, using the geo-atmospheric correction chain PARGE/ATCOR4 (ReSe, 2002). The impact of various processing stages on the recognition of jarosite as well as differences between low and high altitude imagery is investigated.

## 2. IMPACT OF SPATIAL INTERPOLATION ON SPECTRAL ACCURACY

Whenever geometric corrections are performed, image data are to be resampled to a regular grid before the data are stored in a final geometry. This best kind of resampling has already lead to extensive discussions for the geocoding of multispectral satellite imagery. Cubic resampling has been found to lead to the spatially most accurate results for such data, while having a negative impact on the radiometric integrity (Schowengerdt, 1997). For airborne imaging spectrometry, the paradigm so far was to leave the spectra 'as is' in order to avoid interpolated (artificial) spectra in final data products. The arguments for such nearest-neighbor based interpolation are twofold. First, the spectrometric accuracy and spectral uniformity is higher weighted than the spatial accuracy. Second, the interpolation processing of full image data cubes may be very time consuming if, e.g., cubic convolution would be applied to such data. Using an exemplary set of AVIRIS data it has now been tested how various interpolation methods affect the spatial as well as the spectral accuracy of the data.

## 2.1 Methods

The tests performed within this analyses are based on real data sets which have been chosen for proper representation of the errors involved with spatial resampling. The spatial analysis is done in a non-quantitative way by visual comparison of results from resampling options within the geocoding process (see below). The radiometric analysis is done by a method as also described in Schlöpfer et al. 2001.

Six types of resampling are compared:

- nearest neighbor (direct neighbors of the original pixels in a ‘first come first serve’ procedure),
- triangulated nearest neighbor (nearest neighbor with respect to a triangulation of the original pixels),
- across track linear interpolation,
- along track linear interpolation,
- bilinear interpolation (strictly bilinear in two explicit directions), and
- triangulation (equals a multilinear interpolation).

Any higher order interpolations such as ‘cubic convolution’ or ‘quintic interpolation’ (IDL, RSI Inc.) are not further analysed due to their tremendous requirements in processing resources and their high impact on radiometric accuracy. The interpolation methods have been implemented in the parametric geocoding application PARGE.

For the radiometric analysis, four types of masks are used for partial mapping of the data which represent missing individual pixels, missing lines, or groups of missing lines respectively (cf Figure 3). All masked pixels are then replaced by interpolated spectra from the neighboring pixels. Radiometrically equivalent resampling procedures are treated as one (i.e. the two nearest neighbor or the two linear interpolation options). The systematically resampled spectra are then compared to the real spectra at the very same spatial position over masked image areas. The mean relative deviation between the original pixel and the interpolated value is then taken as measure for the error which is related to the interpolation method. For comparison, the maximum relative error is defined as mean deviation of the original spectra under the mask to the average image spectrum. If interpolation results are achieved close to this generic error, the interpolation obviously has failed to create an improved replacement of mis-registered image pixels. The obtained deviations may be interpreted with regard to the resampling of apparent gaps after the geocoding process.

## 2.2 Tests on AVIRIS data

### *Effects on Spatial Pattern*

The spatial effects are investigated on an exemplary low altitude AVIRIS data set from the Navarro River Watershed, Mendocino County, California collected in July 2000 (provided by UC Davis). The results of various interpolation methods are depicted in Figure 1 and Figure 2. Artefacts are evident if the initial geocoding procedure leads to an undersampled image as given in Figure 1. The gaps between the ‘original’ pixels need to be interpolated by the best suited resampling procedure. However, in order to take respect to the argument not to change radiometric measurements, the initial spectra at the center pixel positions are forced to remain unchanged. This oversampled situation is often preferred since it keeps the amount of data losses minimal and usually leads to higher spatial accuracy. If the data amount must be kept minimal while preserving most of the original data, the output grid resolution is taken according to the original image resolution (see Figure 2). Hence, only few pixels are missing after geocoding and need to be replaced.

For the undersampled output grid, it is obvious from Figure 1 that all linear interpolation methods fail to properly reconstruct a realistic spatial pattern in the image. Only a triangulated interpolation can solve the issue satisfyingly. The spatial pattern is also kept if nearest neighbour resampling is applied, but the texture suffers from this kind of resampling by introducing non-realistic ‘crispy’ artefacts. The triangulated nearest neighbor still shows such artefacts although being more accurate by considering triangulated distances between the original pixels. If only few pixels have to be replaced as given in Figure 2, the triangulated interpolation loses its advantage over linear interpolations. A simple and fast linear interpolation can lead to good results, as long as it’s done in across-track direction (for this AVIRIS case example).

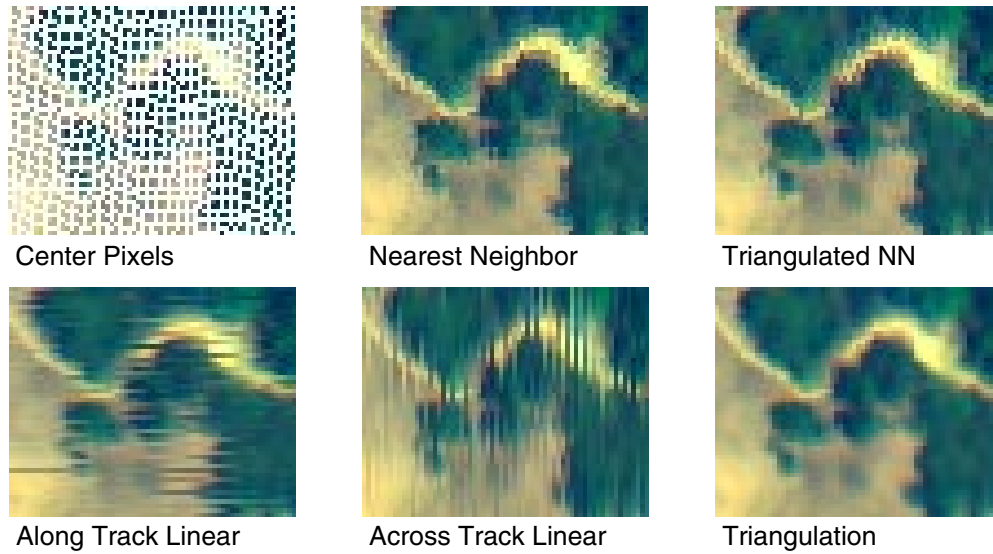


**Figure 1:** Spatial effects of resampling methods in an oversampled grid.

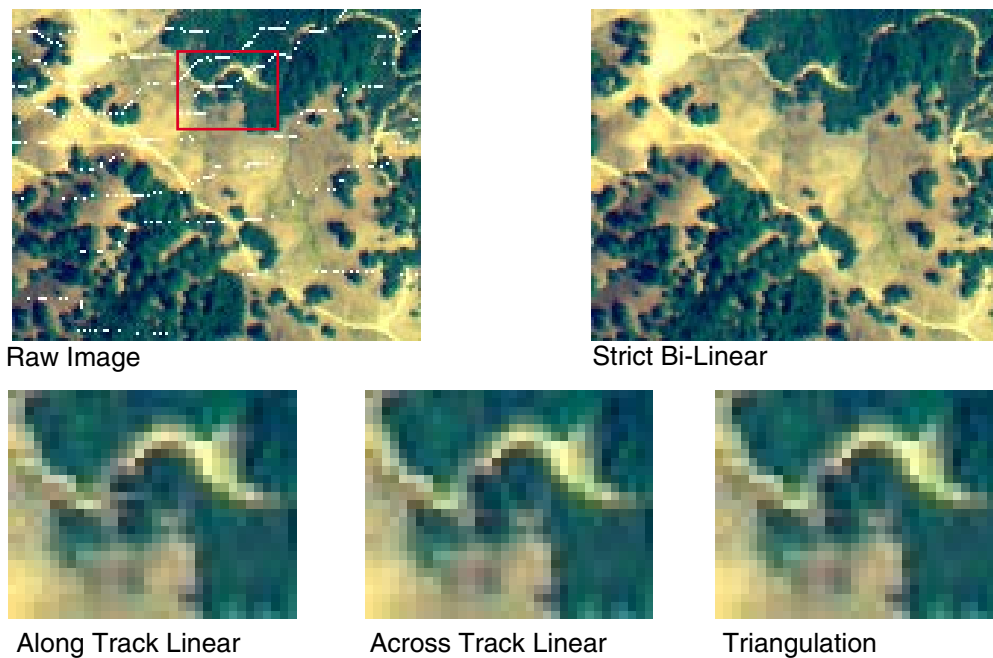


**Figure 2:** Spatial effects of interpolation methods in an equally sampled grid (on AVIRIS data).

### *Radiometric Effects*

The radiometric effects have been investigated with the method as described above. Investigation have been done on a combined AVIRIS low altitude and high altitude data set over the Ray Mine, Arizona, The low altitude data is dating from 10/3/1998 (low altitude) at a nominal ground sampling distance of 3.6 m, while the high altitude dates from 6/5/1998, at a ground sampling distance of 20.2 m.

The radiometric errors due to the applied interpolation are between 5 and 20% for the replacement of single pixels and lines, dependent on the wavelength and the interpolation method (see Figure 3). The peak at lowest wavelengths is directly related to the high noise observed in these bands while the second peak at 680 nm is rather related to the

maximal absorption of vegetation at this wavelength. Bilinear and triangulated interpolation both proved to be superior to nearest neighbor replacement techniques by a factor of 2 in average. The triangulation yields best results if only individual pixels have to be replaced while there is no significant improvement in comparison to linear interpolation for the replacement of whole lines as for masks 2 to 4.

If pixels of a distance higher than the pixel size have to be replaced (i.e. for the black pixels of mask4), the interpolation becomes very inaccurate. The errors are almost on the same level as if the average spectrum would have been taken as interpolated value. For all cases, the nearest neighbor replacement is significantly worse than any other interpolation method. Figure 4 shows that the error in nearest neighbor resampling is almost independent on the mask pattern. The triangulation error on the other hand is only significantly lower than the nearest neighbor-error for the

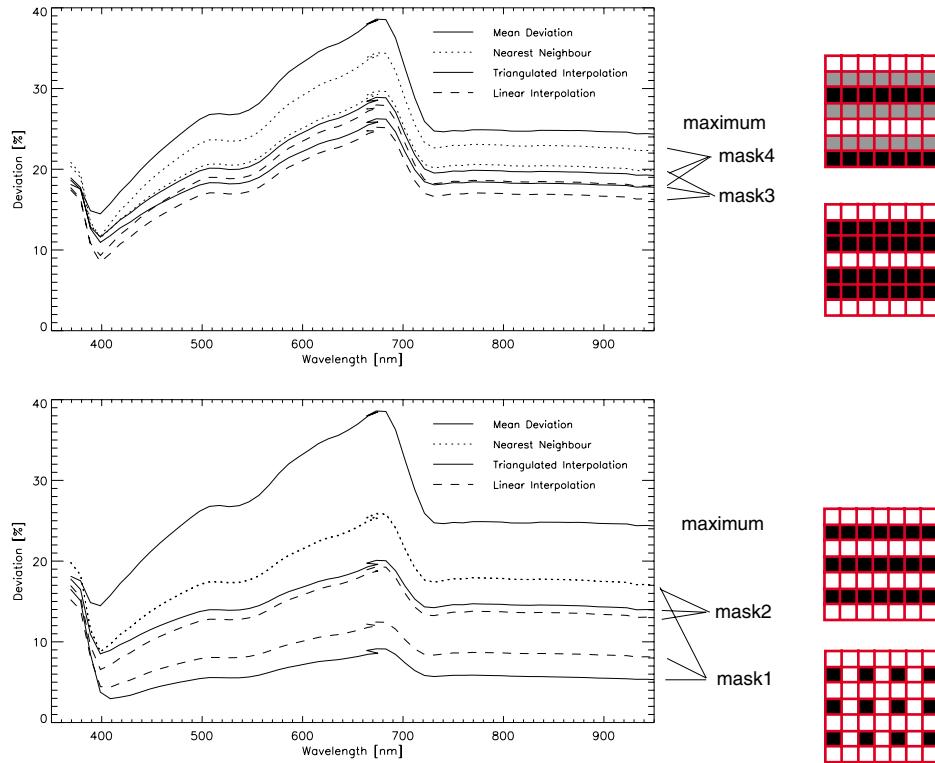


**Figure 3:** Resampling errors for AVIRIS low altitude data in comparison to the maximum error (most upper curve). The upper graphic refers to masks 3 and 4 while the lower graphic refers to masks 1 and 2. The lower lines per interpolation kind correspond to masks 1 and 3, respectively.

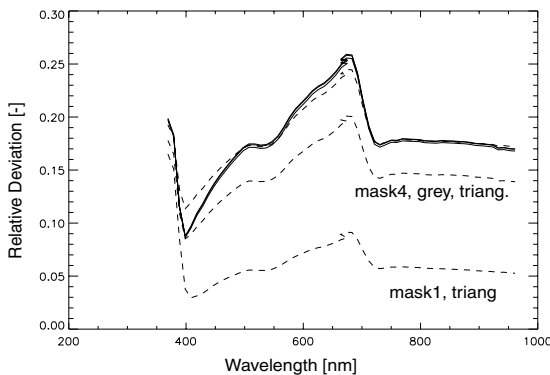


**Figure 4:** Comparison of triangulation (dashed) and nearest neighbor (solid) resampling for mask1 and mask4. The uppermost dashed line corresponds to the black pixels only of mask 4 while the middle dashed line represents the greyed pixels (masks see Figure 3).

replacement of pixels directly adjacent to the original values. However, the relative advantage of triangulation decreases drastically for pixels 'in the second line' (black pixels of mask4 as of Figure 3).

The analysis is extended to AVIRIS high altitude data where the validation is restricted to a reduced number of masks and methods for the intercomparison to AVIRIS low altitude data. Bilinear interpolation can be skipped due to the mask patterns which only allow for interpolations in y-direction. Only 'mask1' has been used for cross comparison of the results between low and high altitude imagery. Figure 5 shows that the absolute deviations are reduced by about one third in comparison to the low altitude data. Nearest neighbor resampling is still viable although the linear interpolation yields better results for the whole wavelength range. The general lower level of errors while interpolating the high altitude data can be explained by the more homogeneous patterns in the imagery at 20 meters resolution in comparison to 4 meters. The scattered vegetation observed in low altitude data is smoothed out and does no longer lead to discontinuities in the imagery.

In general, the best interpolation method leads to an error level of 3-5% for high altitude data, while for low altitude data the error is in a range of 5-10%. This error levels may be attributed to the expected errors for the replacement of individual AVIRIS pixels at an interpolation of 1 pixel distance.

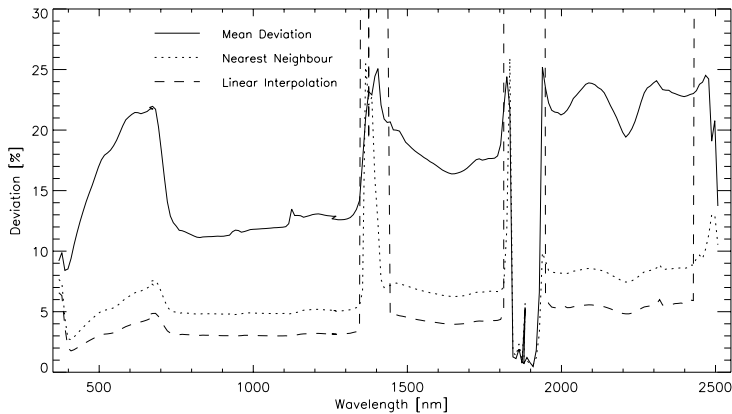


**Figure 5: AVIRIS high altitude results for mask2 and the whole wavelength range.**

### 3. IMPACT OF PREPROCESSING ON SPECTRAL ANALYSIS RESULTS

The second part of this paper summarizes effects of the atmospheric/topographic correction on spectral data analysis methods. Standard methods for data processing include the spectral angle mapper (SAM) or spectral unmixing (SUM). All these methods rely on radiometric comparison of reference spectra from any sources (such as standard reflectance libraries) to the images. Theoretically, such comparison can only be done on a physical basis, if the image data itself has been converted to surface reflectance by atmospheric and topographic correction. The ATCOR4 program has been used to perform the correction of the above-mentioned test data set at Ray Mine, Arizona. The effect of the atmospheric correction on the mean spectrum is given in Figure 6. The engaged atmospheric correction program does not apply any 'spectral polishing' leaving the physically derived reflectance data untouched while terrain effects are reduced. Spectral bands with low atmospheric transmittance (i.e.  $\tau < 0.3$ ) have been eliminated from the data set, since atmospheric correction can not fully compensate such strong distortions. A short analysis showed a high distorting impact if such bands are included in spectral processing methods.

The atmospheric correction of the two datasets over the same spatial extent leads to a minimal relative difference of the retrieved spectra. This fact is illustrated by the example scatterplots in Figure 7. The high altitude and the low altitude image are on a disjunctive data space before applying an atmospheric correction. After the atmospheric correction, both images share the same space. The figure also clearly depicts, that the spectral variation in the high altitude is lower than in the low altitude image of the same area. The data range for the low altitude spectra is significantly larger due to the integrating effect of the larger FOV in the high altitude image.

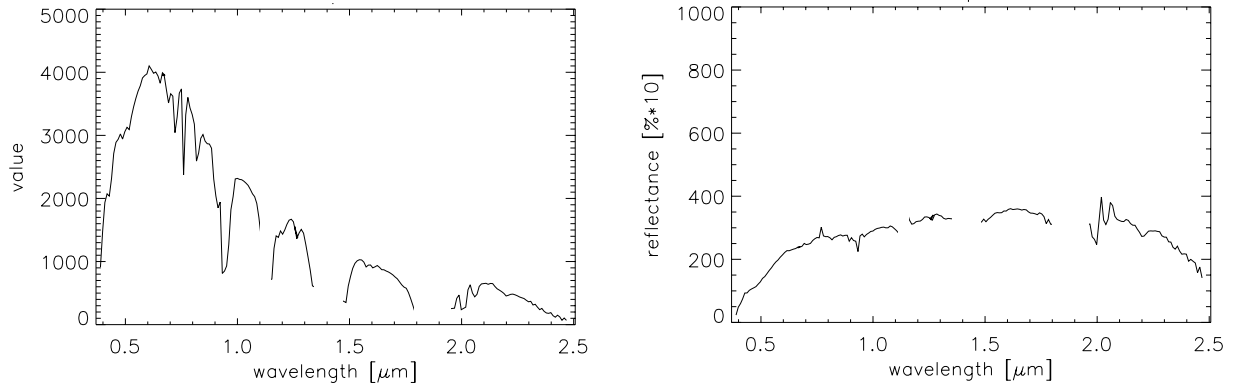


**Figure 6:** Spectral influence of the atmospheric correction on the mean image spectrum. Left: Calibrated and scaled raw AVIRIS imagery, Right: atmospherically corrected. Strong absorbing bands have been mapped out for spectral analysis.

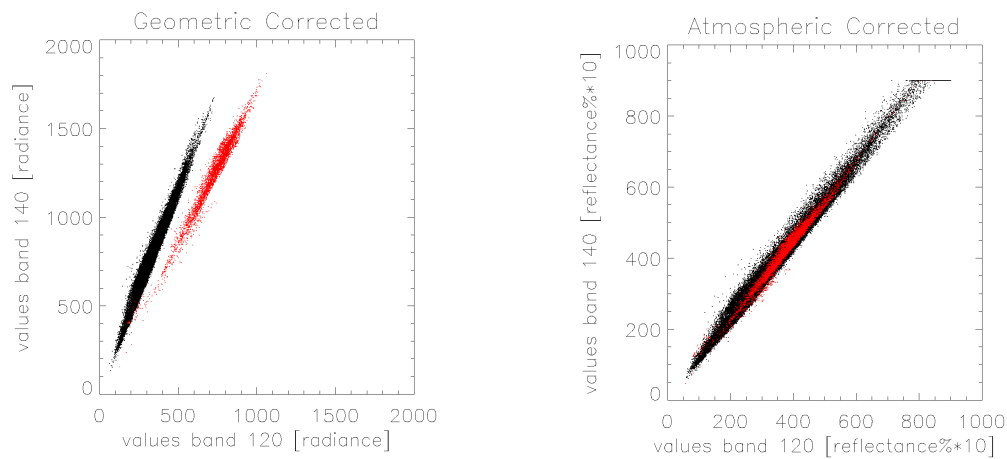


**Figure 7:** Scatterplot of two exemplary spectral bands of the low altitude imagery (black) and the high altitude imagery (red) before and after atmospheric correction.

### 3.1 Spectral Angle Mapper

Spectral angle mapping has been performed for the detection of jarosite using three kind of processing status. The number of detected pixels and the mean spectral angles for these situations are given in Table 1. The high sensitivity of the spectral angle mapping procedure can be illustrated by various facts:

- smallest spectral angles are achieved if the library reflectance spectra are compared to the geo-atmospherically corrected reflectance image,
- the uncertainty in radiative modelling leads to slightly larger spectral angles, if the method is done on at-sensor radiance level instead of reflectance, and
- applying reflectance endmembers directly to the calibrated radiance cube leads to useless results showing SAM angles beyond the necessary accuracy.

The comparison of the low altitude image to the high altitude images (see Figure 8) lead to the following results: in the high altitude image, a far larger number of pixels is classified as jarosite pixels than for the low altitude image at the same constant threshold angle. This is due to the fact that the low altitude image shows larger spectral variations and thus its average spectral angle towards a quite uniform spectrum (as jarosite is) in average are larger. This fact is also underlined by Figure 7, which shows the higher spectral variability in the low altitude image. The case is inverse for SAM on radiance images. The less accurate (or even wrong) radiometry for those cases leads to a higher number of pixels detected in the low altitude image due to its higher variation. The spatial analyses of these results shows that the detected pixels rather depict arbitrary jarosite signals than a consistent mineralogical product.

**Table 1: Differences in number of classified pixels and Spectral Angle between various processing stages and between low altitude and high altitude AVIRIS imagery over the same area. The ‘mean’ angle is calculated within the detected area in relation to the atmospherically corrected low or high altitude image.**

jarosite spectrum	low altitude image match to jarosite [SAM angle, rad] within threshold area	high altitude image match to jarosite [SAM angle, rad] within threshold area
reflectance endmember on atmospheric corrected reflectance image	<i>threshold=0.09:</i> mean = 0.089; #pixels: 37 <i>threshold=0.10:</i> mean = 0.096; #pixels: 4 649	<i>threshold=0.09:</i> mean = 0.082. #pixels: 25 959 <i>threshold=0.10:</i> mean = 0.087; #pixels: 88 228
reflectance endmember on geometric correcte calibrated radiance image	<i>threshold=0.74:</i> mean = 0.222; #pixels: 2 955 <i>threshold=0.80:</i> mean = 0.190; #pixels: 14 229	<i>threshold=0.74:</i> no values detected <i>threshold=0.80:</i> mean = 0.176; #pixels: 3 296
simulated radiance endmember on geometric correcte calibrated radiance image (indirect)	<i>threshold=0.10:</i> mean = 0.138; #pixels: 643 <i>threshold=0.13:</i> mean = 0.122; #pixels: 36 677	<i>threshold=0.10:</i> no values detected <i>threshold=0.13:</i> mean = 0.089; #pixels: 495

### 3.2 Spectral Unmixing

The robustness of the linear spectral unmixing approach has been tested on the atmospherically corrected image. The selected concurrent endmember minerals to jarosite are kaolinite, hematite, and goethite. The latter represents a dark mineral with flat spectral characteristics (a suited spectrum instead of a ‘shadow’ endmember). Figure 8 shows a larger area detected in the high altitude images than in the low altitude image under the same prerequisites for both SAM and SUM classification. While for the SAM classification the detected area grows vastly, the detected are in the SUM are growin moderately but are almost disjunctive between the low altitude and the high altitude image. The effect of spatial resolution is stronger in the spectral angle mapper than in spectral unmixing. The concurrent endmembers in the SUM limit the difference due to resolution changes whereas the SAM only displays relative differences between one endmember and the real spectrum.

Discrepancies between low and high altitude images are also found to origin in the time delay between the two images, being about 4 months. During this time period, the surface has changed significantly in this active mining district. The dust roads (e.g.) are almost completely differently mapped by the two methods. This is assumed to be a temporal change detected in that area which is obvious in the true color images of the critical area. Anyhow, the differences between SUM and SAM unmixing are significant and still are not completely understood.

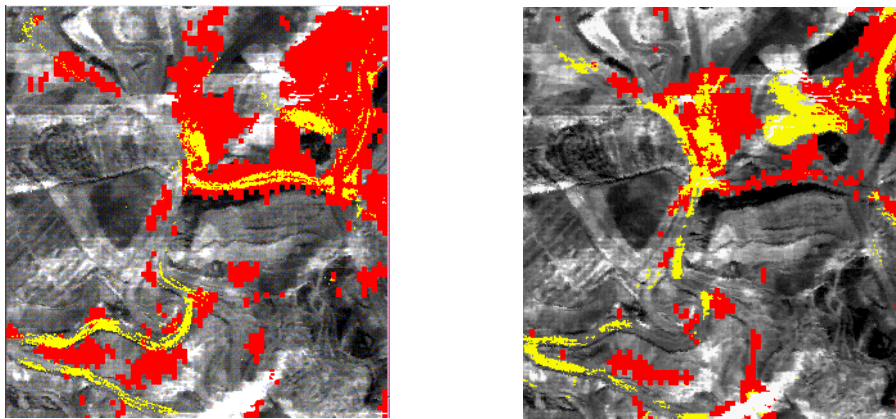


**Figure 8: Differences in detected jarosite pixels using the spectral angle mapper (left) and the linear spectral unmixing (right) on low altitude imagery (yellow) and high altitude imagery (red).**

## 4. CONCLUSIONS

The described experiments give an order of magnitude for the expected errors if interpolations need to be done in spectral processing and if the 'same' spectral analysis is done on various kind and processing status of spectral data. The results point towards important issues to be considered in data preprocessing. The radiometric analysis of spatial interpolation processes questions an often-heard paradigm in imaging spectroscopy that no 'artificial' spectra shall be produced by using interpolations. A significant higher error in the spectra derived by nearest neighbour resampling is observable in comparison to other interpolation methods. Thus, linear interpolations can be recommended for the replacement of individual pixels or missing lines. Furthermore, it has been shown that the replacement of pixels outside the reach of the pixel PSF is very questionable and should be avoided wherever possible. The choice of interpolation method depends on the target grid resolution. For undersampled grids, triangulated interpolation leads to superior results, while for regularly sampled grids the more efficient linear interpolations are sufficient.

The short analysis of spectral unmixing and spectral angle mapper methods for the detection of jarosite in an open pit mine showed, how heavily radiometric effects can influence the results of spectroscopic analysis. It is indicated that the preprocessing status as well as the spatial resolution of the image have a significant impact on the discernability of abundant minerals in geological imaging spectroscopy. The mineral detection can completely be distorted, if no attention is paid towards processing status and quality of the input data. Stability of both, spectral unmixing and spectral angle mapping proved to be critical towards atmospheric preprocessing, number of spectral bands, as well as spatial resolution. These issues may be solved by careful tuning of the spectral analysis methods using absolute reflectance data corrected to hemispherical reflectance units (including approximate corrections for BRDF effects).

The values have been derived from exemplary real imaging spectrometer data and thus are only of limited generic validity. Anyhow, the results of this analysis will be used to improve the capabilities of current geo-atmospheric processing systems such as PARGE and ATCOR4. On the geometric side, flexible options for interpolation of imaging spectrometry data in the processing chain need to be provided to the data users. On the radiometric side, the importance of highest accuracy atmospheric and topographic corrections for consistent results in imaging spectroscopy applications once more has been illustrated.

## 5. ACKNOWLEDGEMENTS

Part of this work has been supported by the ESA/ESTEC contract 14906/00/NL/DC. NASA/JPL and the AVIRIS team is thanked for providing the AVIRIS 1998 data and Carlos Ramirez of the UC Davis is thanked for providing some of the more recent AVIRIS data examples.

## 6. REFERENCES

- ReSe, 2002: PARGE v1.3.4, ATCOR4 v2.1, distributed by ReSe Applications Schläpfer, software available from <http://www.rese.ch>.
- Richter R., 1997: Correction of atmospheric and topographic effects for high spatial resolution satellite imagery. *Int. J. Rem. Sens.*, 18(13):1099-1111.
- Richter, R., 2000: *Atmospheric / Topographic Correction for Wide FOV Airborne Imagery: Model ATCOR4*. DLR Internal Report, DLR-IB 552-05/00, Wessling, Germany, pp. 62.
- Schläpfer D., Schaepman M., and Itten K.I., 1998: PARGE: Parametric Geocoding Based on GCP-Calibrated Auxiliary Data. Descour, M.R. and Shen, S.S. (Eds.), *Imaging Spectrometry IV*, SPIE, San Diego, Vol. 3438:334-344.
- Schläpfer D., Schaepman M., and Strobl P., 2001: Impact of Spatial Resampling Methods on the Radiometric Accuracy of Airborne Imaging Spectrometer Data. 5th Int. Airb. R. S. Conf. and Exh., VERIDIAN, San Francisco / Miami, CD-ROM, pp.8.
- Schowengerdt R.A., 1997: *Remote Sensing: Models and Methods for Image Processing*. Academic Press, 2nd Ed., pp. 522.